JPET Fast Forward. Published on December 27, 2019 as DOI: 10.1124/jpet.119.263152
This article has not been copyedited and formatted. The final version may differ from this version.

Title Page

From genotype to phenotype: content and activities of cytochromes P450 2A6 in huma n liver *in vitro* and predicted *in vivo*

Authors and Affiliations

Yan Fang[1], Tong Wang[1], Yuan-Yuan Guo[1], Hai-Feng Zhang[1], Qiang Wen[1], Yu-Rong Xing[2*], Na Gao[1*]， Hai-Ling Qiao[1*]

[1]Institute of Clinical Pharmacology, Zhengzhou University, Zhengzhou 450052, Henan, China

[2]Center of Health Examination, The First Affiliated Hospital of Zhengzhou University, Zhengzhou450052, Henan, China

JPET Fast Forward. Published on December 27, 2019 as DOI: 10.1124/jpet.119.263152
This article has not been copyedited and formatted. The final version may differ from this version.

Running Title Page

Running title

Genotype to phenotype: CYP2A6 *in vitro* and *in vivo*

*Corresponding author: Hai-Ling Qiao (qiaohl@zzu.edu.cn). No 40, Daxue Road, Erqi District, Zhengzhou City, Henan Province, China.Tel:+86-0371-6665-8363. Fax: +86-0371-6665-8363

Additional corresponding author: Na Gao (gaonawe@zzu.edu.cn), Yu-Rong Xing (405274775@qq.com)

Number of text pages: 44

Number of tables: 2

Number of figures: 6

Number of references: 46

Number of words in the Abstract: 237

Number of words in the Introduction: 749

Number of words in the Discussion: 1379

Keywords: CYP2A6; genotype-phenotype; intra-individual variation; inter-individual variation; coumarin; *in vitro-in vivo* extrapolation;

Abbreviations

CYP2A6; cytochrome P4502A6; HLM, human liver microsomes; ICV, intra-individual percentage coefficient of variation.

JPET Fast Forward. Published on December 27, 2019 as DOI: 10.1124/jpet.119.263152
This article has not been copyedited and formatted. The final version may differ from this version.

Abstract

Unraveling the molecular mechanisms by which genetic variants of cytochrome P450 2A6 (CYP2A6) lead to different metabolic phenotypes remains a long-standing but important challenge. CYP2A6 is an enzyme involved in the metabolism of several clinical drugs as well as the metabolic activation of carcinogenic nitrosamines. Herein, *CYP2A6* genotypes and phenotypes, as indicated by protein content (by LC-MS/MS) and metabolic activities (V_{max}, CL), were determined for 90 human liver samples. We determined the median, range, and inter-individual and intra-individual variation of CYP2A6 content and activity at the microsomal, liver tissue, and whole liver level and predicted hepatic *in vivo* clearance by *in vitro-in vivo* extrapolation based on CYP2A6-mediated coumarin metabolism by each *CYP2A6* genotype. These results reveal how different *CYP2A6* genotypes yield different phenotypic traits in protein content and enzyme activity. For relative V_{max}, CL and protein content, the intra-individual percentage coefficients of variation (ICVs) were 41.0% (18.8-125.1%), 28.5% (2.39-133.5%) and 27.8% (2.68-88.0%), respectively. The high ICVs implied large intra-individual variation at different levels, sometimes in a genotype-dependent manner. Inter-genotype analysis revealed that the *CYP2A6*4* allele demonstrated the most obvious effect on phenotypic outcomes, both in protein content and in metabolic activity. Indeed, decreased CYP2A6 protein content with the *CYP2A6*4* genotype might explain the decreased metabolic activity from the molecular to the organismal level. These findings may allow useful predictions for CYP2A6-mediated drug metabolism on an individual patient basis in accord with the goal of achieving personalized medicine.

JPET Fast Forward. Published on December 27, 2019 as DOI: 10.1124/jpet.119.263152
This article has not been copyedited and formatted. The final version may differ from this version.

Significance Statement

We provide the median, range, and inter-individual and intra-individual variation in CYP2A6 content at the microsomal, liver tissue, and whole liver level by LC-MS/MS as well as activities at the protein, microsomal, liver tissue, and whole liver level both *in vitro* and at the organismal level based on CYP2A6-mediated coumarin metabolism with each CYP2A6 *genotype*, thereby allowing us to elucidate how different *CYP2A6* genotypes yield differing phenotypic traits (protein content and enzyme activity), facilitating the development of personalized medicine.

JPET Fast Forward. Published on December 27, 2019 as DOI: 10.1124/jpet.119.263152
This article has not been copyedited and formatted. The final version may differ from this version.

Introduction

A recent study (Tennessen et al., 2012) yielding the sequence of 15,585 human protein-coding genes showed that 2.3% of the 13,595 single nucleotide variants, involving ~313 genes were predicted to impact protein function. Cytochrome P450 (CYP) enzymes are characterized by abundant gene polymorphisms and great inter-individual variations in drug metabolizing activity (Zanger and Schwab, 2013). Our previous studies, carried out with human liver samples derived from both normal and hepatocellular carcinoma (HCC) individuals indicated that various genetic variants of *CYP450* (Gao et al., 2016b; Fang et al., 2018a; Fang et al., 2018b) combined with other factors including CYPOR (Tian et al., 2016; Fang et al., 2018b) and CYPb5 (Zhang et al., 2015a) generated significant variation in metabolic phenotypes (Gao et al., 2017c; Zhang et al., 2016).

More importantly, differences in CYP activity (Gao et al., 2016a; Zhou et al., 2016), are associated with increased risk for diseases like hepatofibrosis (Gao et al., 2017b) and hepatocarcinogenesis (Gao et al., 2018a; Gao et al., 2018b). Thus, studies on *CYP* genotype-phenotype associations may have important disease implications. However, with regard to metabolic phenotypes for CYPs, research in this area has focused primarily on the effect of *CYP* genetic variants on enzyme-catalyzed drug metabolism *in vitro* (Palma et al., 2010; Murdter et al., 2012; Dai et al., 2014; Werk and Cascorbi, 2014) or on drug clearance *in vivo* (Mega et al., 2009; Zordoky and El-Kadi, 2010; Zhu et al., 2011; Shuker et al., 2016). It has long been known that genetic effects on physiological phenotypes often depend on the cellular and environmental context, such as culture media, cell type, or tissue. For this reason, a more comprehensive process for *CYP* genotype-phenotype association is needed.

JPET Fast Forward. Published on December 27, 2019 as DOI: 10.1124/jpet.119.263152
This article has not been copyedited and formatted. The final version may differ from this version.

In the past several years, CYP2A6 has gained importance in numerous studies on the more than 45 known allelic variants (http://www.imm.ki.se/CYPalleles/cyp2a6.htm) and their roles in the metabolism of coumarin and a number of pharmaceuticals. Along with these pharmaceuticals, toxins and procarcinogens such as aflatoxin B1 and tobacco-specific nitrosamines may exhibit differences in blood concentration and duration of effect as a result of *CYP2A6* polymorphisms (Xu et al., 2002; Sadeque et al., 1997; White et al., 2001) that are metabolically activated by CYP2A6. Development of a comprehensive genotype–phenotype model for CYP2A6 has the potential to improve our understanding of phenotypic variation and enhance the prediction of clinical outcomes for drugs metabolized by this P450.

Clinically, studies on *CYP2A6* genotype-phenotype associations may have important clinical implications due to its major role in the metabolism of nicotine. However, studies on *CYP2A6* genotypes determined *in vitro* (Fukami et al., 2005; Wang et al., 2006) (e.g. by site-directed mutagenesis and liver microsomes) and/or *in vivo* (e.g. by phenotyping using substrates) are not always consistent. Take *CYP2A6*1B* as example: it was characterized with either elevated catalytic activity (Yoshida et al., 2003; Wang et al., 2006) or normal activity (Ujjin et al., 2002; Peamkrasatam et al., 2006; Wang et al., 2011), making it difficult to determine the genotype-phenotype association and predict phenotypic outcomes.

One recent report focused on the CYP2A6 genotype-phenotype correlation and showed large inter-individual variation in phenotypes (Tanner et al., 2017). Unfortunately, insufficient background information for more than half of the donors made accurate and rigorous evaluation of the genotype-to-phenotype association difficult. Moreover, phenotypes including protein content and activity measured in

that study were only determined at one level *in vitro*. The extrapolation from phenotype *in vitro* to phenotype *in vivo* is complex and may involve multiple intermediates. Simple genotype-to-phenotype prediction may not be sufficient to accurately determine the phenotype. As a result, efforts to identify the influential intermediate steps in the process from genotype to ultimate phenotype for CYP2A6 are still an urgent need.

With regard to the characterization of CYP2A6 phenotypes, as mentioned in a previous study (Gao et al., 2017a), they can be divided into content phenotypes and metabolic phenotypes, as evidenced by CYP2A6 protein expression and activity from the molecular level to the cellular level, and then to organismal level.

We generated a genotype-phenotype model for CYP2A6 based on three gene polymorphisms of *CYP2A6* (*CYP2A6*1B, *4* and **9*) with frequencies greater than 1% in Chinese subjects. We determined protein expression and metabolic activity from the molecular to the cellular (microsomal, liver tissue and liver), and organismal level, and present the intra-individual and inter-individual variation in metabolic activity for CYP2A6 with different genotypes. Consideration of differences in enzyme activity at the molecular level and the effect on clearance at the organismal level may provide insight into how *CYP2A6* molecular genetic variation influences phenotypic variation.

Material and methods

Human Liver Samples

Normal human liver tissues were obtained from 90 Chinese patients undergoing

liver surgical resection at Henan Provincial People's Hospital or Henan Provincial Tumor Hospital during 2012 and 2014. This research was performed in accordance with the Declaration of Helsinki. All experiments were approved by the Medical Ethics Committee of Zhengzhou University, and written informed consent was obtained from all patients. All liver samples were obtained from patients undergoing hepatic surgery and were free of infectious disease, with medical diagnoses mostly of cavernous hemangioma of liver (61 cases); a few were from metastatic cancers (7 cases), cholelithiasis (8 cases), gallbladder cancer (4 cases), hepatic cholangiocarcinoma (6 cases), or hepatocellular carcinoma (4 cases). Detailed demographic information for the liver samples are presented in Supplemental Table 1. For tumor-bearing patients, normal liver samples were obtained 2 cm distant from the tumor tissue. Liver function tests, histopathological analysis and imaging by ultrasonography or CT were used to confirm that only liver tissue with normal liver function and normal histological appearance was collected. Liver samples were frozen immediately after removal and stored in liquid nitrogen until use. No history of exposure to known CYP-inducing or inhibiting agents and only routine anesthetics were used with the patients. Detailed donor characteristics of the human liver samples and human liver microsomes (HLMs) and the method of preparation by differential centrifugation are described in a previous study (Zhang et al., 2015b). Total HLM protein concentration was measured by the Bradford method (Bradford, 1976).

Genotyping of CYP2A6

Genomic DNA was isolated from human liver tissues using a genomic DNA purification kit (Beijing ComWin Biotech Co.,Ltd., China). A two-step PCR method (Oscarson et al., 1999) was used to detect *CYP2A6*1B* and *CYP2A6*4*. Another SNP *CYP2A6*9* (rs28399433) was genotyped by PCR sequencing. Genotyping errors were

JPET Fast Forward. Published on December 27, 2019 as DOI: 10.1124/jpet.119.263152
This article has not been copyedited and formatted. The final version may differ from this version.

detected by re-genotyping with a sub-sample and reproducibility was routinely greater than 99%.

Quantification of CYP2A6 protein

Protein quantification of CYP2A6 was performed by nano-LC-MS/MS as previously reported (Zhang et al., 2016). A QconCAT protein consisting of 57 stable isotope-labeled peptides from 21 drug metabolizing enzymes (including CYP2A6) in which two or three peptides were selected for each targeted protein was employed to quantify these proteins in HLMs (Li et al., 2015). The concentration of CYP2A6 protein was determined by nano-LC-multiple reaction monitoring MS using an easy nano-LC (Thermo Fisher Scientific Inc., Waltham, MA, USA) coupled to a TSQVantage^{TM} Triple Quadrupole mass spectrometer (Thermo Fisher Scientific Inc.).

Determination of phenotype at different levels

Molecular phenotype is defined as protein content ($Content_{-P}$) and activity (V_{max-P}, CL_{-P}) at the protein level. Cellular phenotype can be divided into microsomal, tissue and organ levels; Accordingly, protein expression at the cellular level in the liver is defined as $Content_{-M}$, $Content_{-LT}$, $Content_{-L}$, and activity is defined as V_{max-M}, V_{max-LT}, V_{max-L} and CL_{-M}, CL_{-LT}, CL_{-L}, respectively. For organismal phenotype, this refers to drug clearance from the body at the whole organism level (*in vivo*).

Microsomal phenotype. The sub-cellular phenotype, termed the microsomal phenotype, is defined as protein content (CYP_{-M}), V_{max} (V_{max-M}) and clearance (CL_{-M}). V_{max-M} and CL_{-M} were determined by measuring the rate of coumarin 7-hydroxylation by high performance liquid chromatography with eight coumarin concentrations (0.156-20 μM) according to a previously described method (Zhang et al., 2016). Incubation mixtures contained HLMs, 100 mM phosphate buffer (pH 7.4) with 1 mM

NADPH and substrate. Optimal protein concentration was 0.3 mg/ml protein and incubation time was 30 min. Perchloric acid (10 μl) was added to terminate the reaction. The metabolite was identified by HPLC-UV. All experiments included two replicates. The Michaelis–Menten constant (K_m) and maximum reaction rate ($V_{max\text{-}M}$) of CYP2A6 was determined by nonlinear regression analysis using GraphPad Prism 6.0 and $CL_{\text{-}M}$ was calculated based on the ratio of $V_{max\text{-}M}$ to K_m.

$$CL_{\text{-}M} = V_{max\text{-}M} / K_m \qquad \text{(Eq. 1)}$$

Molecular phenotype. The metabolic phenotype at the molecular level is defined as V_{max} ($V_{max\text{-}P}$) and clearance ($CL_{\text{-}P}$) of drug per pmol of CYP2A6. The $V_{max\text{-}P}$ and $CL_{\text{-}P}$ for each individual was obtained by dividing each individual microsomal phenotype parameter by the corresponding individual CYP2A6 protein content ($Content_{\text{-}M}$).

$$CL_{\text{-}P} = CL_{\text{-}M} / Content_{\text{-}M} \qquad \text{(Eq. 2)}$$

Tissue phenotype. The tissue phenotype is defined as protein content ($Content_{\text{-}LT}$), V_{max} ($V_{max\text{-}LT}$) and clearance ($CL_{\text{-}LT}$). The $Content_{\text{-}LT}$, $V_{max\text{-}LT}$ and $CL_{\text{-}LT}$ for each individual was obtained by multiplying each individual microsomal phenotype parameter ($Content_{\text{-}M}$, $V_{max\text{-}M}$ and $CL_{\text{-}M}$) by the corresponding individual MPPGL. MPPGL is the microsomal protein per gram of liver and determined as previously reported (Zhang et al., 2015b). The mean MPPGL value was 42.0 (9.9–127.9) mg/g in this cohort of 90 liver samples.

$$CL_{\text{-}LT} = CL_{\text{-}M} \times MPPGL \qquad \text{(Eq. 3)}$$

Organ phenotype. The organ phenotype is defined as content ($Content_{\text{-}L}$), V_{max} ($V_{max\text{-}L}$) and clearance ($CL_{\text{-}L}$) in liver. $Content_{\text{-}L}$, $V_{max\text{-}L}$ and $CL_{\text{-}L}$ were obtained by multiplying each individual LW/BW by the individual tissue phenotype parameter,

JPET Fast Forward. Published on December 27, 2019 as DOI: 10.1124/jpet.119.263152
This article has not been copyedited and formatted. The final version may differ from this version.

also known as Content$_{\text{-LT,}}$ $V_{max\text{-}LT}$ and $CL_{\text{-LT,}}$ respectively. Detailed values of LW and BW were previously reported (Gao et al., 2017a). BW is the actual body weight (BW) for each individual and LW is the liver weight, which is calculated by multiplying the liver volume (LV) by the liver density, where LV (ml)=12.5 × BW (kg)+536.4 (Wang et al., 2008) and the liver density is 1.001 g/ml (Yuan et al., 2008). The mean LW/BW value was 21.2 (18.4–30.4) g/Kg in this cohort of 90 liver samples.

Organismal phenotype. The organismal phenotype is defined as clearance ($CL_{\text{-H}}$) *in vivo*. According to our previous report, the Bias-Corrected Conventional *in vitro-in vivo* extrapolation method (Gao et al., 2016a; Gao et al., 2017a) was adopted for extrapolating the $CL_{\text{-H}}$ for different genotypes on the basis of Q_H, $f_{u,p}$ and R_B. C_O, the cardiac output (C_O), determined based on age and gender, was 5.45 (4.92–6.65) L/min. Q_H， the hepatic blood flow, determined as 24.5% of the C_O (Barter et al., 2013), was 1334.9 (1205.4–1629.3) ml/min. The plasma unbound fraction, $f_{u,p}$, determined as 0.055 for coumarin and R_B, ratio of the drug concentration in blood to plasma, determined as 1 for coumarin, were obtained from our previous study (Gao et al., 2016a). Detailed data and the computing method for Q_H, $f_{u,p}$ and R_B were reported in our previous studies (Zhang et al., 2015b; Gao et al., 2016a). The clearance for CYP2A6 *in vivo* ($CL_{\text{-H}}$) was calculated using the well-stirred model:

$$CL_{\text{-H}} = (Q_H \times CL_{\text{-L}} \times f_{u,p} / R_B) / (Q_H + CL_{\text{-L}} \times f_{u,p} / R_B) \quad \text{(Eq. 4)}$$

The average fold-error (AFE) was introduced to assess the overall accuracy of prediction, which was calculated as follow:

$$AFE = 10^{\frac{1}{N} \sum \log(\text{predicted mean} / \text{observed overall mean})} \quad \text{(Eq. 5)}$$

The individual fold-error (IFE) was introduced to evaluate the individual

JPET Fast Forward. Published on December 27, 2019 as DOI: 10.1124/jpet.119.263152
This article has not been copyedited and formatted. The final version may differ from this version.

accuracy, which was calculated as:

$$\text{IFE} = 10^{\frac{1}{N}\sum \log(\text{predicted individual value} / \text{observed overall mean})} \quad \text{(Eq. 6)}$$

N refers to the number of separate reports in the literature concerning coumarin intravenous clearance.

The definitions and corresponding units for parameters at each level were listed in Table 1.

Intra-individual variation of CYP2A6 at different levels

To make CYP2A6 phenotypes at different levels comparable, relative V_{max} ($R_{\text{-Vmax}}$), relative CL ($R_{\text{-CL}}$) and relative Content ($R_{\text{-Content}}$) were computed. For one specific level, $R_{\text{-Vmax}}$, $R_{\text{-CL}}$ and $R_{\text{-Content}}$ were calculated as the individual V_{max}, CL and Content divided by the median for that level. Variation in $R_{\text{-Vmax}}$, $R_{\text{-CL}}$ and $R_{\text{-Content}}$ among different levels for each person was expressed as the intra-individual percentage coefficient of variation (ICV).

Relative phenotypes ($R_{\text{-Vmax}}$, $R_{\text{-CL}}$ and $R_{\text{-Content}}$) = (individual value) / (median) (Eq. 7)

ICV for relative phenotypes = (standard deviation) / (average value) (Eq. 8)

For one specific relative phenotype ($R_{\text{-Vmax}}$, $R_{\text{-CL}}$ or $R_{\text{-Content}}$), the ICV was calculated as the standard deviation divided by the corresponding average value of the relative phenotype among different levels.

To compare the variation trend of V_{max} and CL from the molecular to the organismal level, the percentage rank change of individual CYP2A6 phenotypes was developed. Ninety samples were ranked in ascending order according to the value of

JPET Fast Forward. Published on December 27, 2019 as DOI: 10.1124/jpet.119.263152
This article has not been copyedited and formatted. The final version may differ from this version.

each metabolic phenotype parameter $V_{max\text{-}P}$, $V_{max\text{-}M}$, $V_{max\text{-}LT}$, $V_{max\text{-}L}$, $CL_{\text{-}P}$, $CL_{\text{-}M}$, $CL_{\text{-}LT}$, $CL_{\text{-}L}$ and $CL_{\text{-}H}$. The rank change for each individual was determined by comparison with phenotype at the molecular level ($V_{max\text{-}P}$ or $CL_{\text{-}P}$), by calculating the absolute difference value between the rank of V_{max} or CL at different levels ($V_{max\text{-}M}$, $V_{max\text{-}LT}$, $V_{max\text{-}L}$, or $CL_{\text{-}M}$, $CL_{\text{-}LT}$, $CL_{\text{-}L}$, $CL_{\text{-}H}$) and the rank of corresponding $V_{max\text{-}P}$ or $CL_{\text{-}P}$. The percentage of rank change was computed for the sum of the 90 samples divided by the rank change absolute value of each individual. For CYP2A6 content, content phenotype at the molecular level could not be obtained, so analysis of its rank change could not be determined.

Inter-genotype variation of CYP2A6 at different levels

$V_{max\text{-}P}$, $V_{max\text{-}M}$, $V_{max\text{-}LT}$, $V_{max\text{-}L}$, $Content_{\text{-}M}$, $Content_{\text{-}LT}$, $Content_{\text{-}L}$, $CL_{\text{-}P}$, $CL_{\text{-}M}$, $CL_{\text{-}LT}$, $CL_{\text{-}L}$, $CL_{\text{-}H}$ were sorted by CYP2A6 genotype. As compared with wild-type, fold-changes of genotype was calculated by dividing the absolute value of the median for the phenotype by the absolute value of median for the corresponding wild-type. The fold-change for all phenotypes with wild-type were defined as one.

Statistical Analysis

Statistical analysis was performed using SPSS 22.0 software (SPSS Inc., Chicago, IL, USA). Kolmogorov-Smirnov and Shapiro-Wilk tests were introduced to assess the normality of the data distribution. One-way ANOVA and Bonferroni tests were used for the comparison of relative phenotype potency. Since most data sets of phenotypes, including kinetic parameters and protein content were not normally distributed, non-parametric methods were generally used. Mann-Whitney U and Kruskal-Wallis H tests were used for pairwise comparison and multiple pairwise comparisons of phenotypes with different genetic polymorphisms. Non-parametric

JPET Fast Forward. Published on December 27, 2019 as DOI: 10.1124/jpet.119.263152
This article has not been copyedited and formatted. The final version may differ from this version.

Spearman rank correlation analysis was conducted to calculate the correlation coefficient (r) among different phenotypes. $P<0.05$ (two-tailed) was considered statistically significant. Graphs were generated using Graph Pad Prism software version 6.02. Both the genotyping and phenotyping tests were derived from three separate and independent replicates to obtain an accurate value. Experimental results were averaged to obtain a single value for that experimental series.

Results

Genotype of CYP2A6

The three most common genetic variants with an allele frequency of more than 1% in the Chinese population were analyzed for a total of 90 samples. The allele *CYP2A6*1B* has a gene conversion located in the 3'-UTR, with the frequency of the wild-type, heterozygous and homozygous genotypes being 12.22%, 56.67%, 17.78%, respectively. *CYP2A6*4* is a *CYP2A6* gene deletion variant, with the frequency of the wild-type and heterozygotes being 86.67% and 13.33%, respectively, and no homozygous genotype detected. The *CYP2A6*9* (-48T>G) is located in the TATA box, with the frequency of the wild-type, heterozygous, and homozygous genotype being 51.11%, 32.22% and 3.33%, respectively.

Phenotype of CYP2A6

Phenotypes at different levels. Substantial inter-individual variations in the metabolic phenotypes (V_{max}, CL) and protein phenotypes (Content) for CYP2A6 from the molecular to cellular, then to organismal levels are depicted in Table 2, with the greatest difference in CL (454-fold) at microsomal level, 144.8 (1.20~544.7) μl/min/mg. The CL phenotype exhibited the most remarkable variations, followed by

JPET Fast Forward. Published on December 27, 2019 as DOI: 10.1124/jpet.119.263152
This article has not been copyedited and formatted. The final version may differ from this version.

V_{max}, and CYP2A6 content was relatively smaller at most levels. Variations of V_{max} showed an increased trend from molecular (63.8-fold) to the tissue level (247-fold), then to the organ level (134-fold).

To make CYP2A6 phenotypes at different levels comparable, relative V_{max} (R-$_{Vmax}$), CL (R-$_{CL}$) and Content (R-$_{Content}$) were computed. Each level's R-$_{Vmax}$, R-$_{CL}$ and R-$_{Content}$ were calculated as the individual V_{max}, CL and Content divided by the median for that level. To sort each level's relative phenotypes in a strong-to-weak sequence, we evaluated the relative potencies at each level (R-$_{Vmax,}$ R-$_{CL,}$ R-$_{Content}$) in 90 samples. It is noteworthy that the R-$_{Vmax}$ potencies at the organ (liver) level, compared with other levels, were always higher. Analysis for the values of R-$_{Vmax}$ of four different levels revealed that the R-$_{Vmax}$ for the organ level was significantly higher than that of the other 3 levels (Table 2). For values of R-$_{CL}$ and R-$_{Content}$, statistically significant differences were not demonstrated among different levels.

Intra-individual variation among different levels. The relative V_{max} (R-$_{Vmax}$), CL (R-$_{CL}$) and Content (R-$_{Content}$) values for different levels are depicted in Fig. 1. The ICVs (intra-individual percentage coefficient of variation) of R-$_{Vmax,}$ R-$_{CL,}$ R-$_{Content}$ within different levels were 41.0% (18.8-125.1%), 28.5% (2.39-133.5%), and 27.8% (2.68-88.0%) for 90 cases (Fig. 1A). ICV with the value >100%, 50-100% and <50% is indicative of high, moderate and low variation, respectively. In these 90 cases, the number (percentage) of high, moderate and low ICV for the values of R-$_{Vmax}$ within four levels was 4 (4.44%), 10 (11.1%) and 76 (84.4%); for R-$_{CL}$, it was 4 (4.44%), 24 (26.7%) and 62 (68.9%); while for R-$_{Content}$, it was 15 (16.7%), 75 (83.3%) for moderate and low ICV, respectively; no high ICV was detected. The results indicated surprisingly high intra-individual variation for CYP2A6 phenotypes among different levels. When relative phenotypes were classified by *CYP2A6* genotypes, the ICVs of

JPET Fast Forward. Published on December 27, 2019 as DOI: 10.1124/jpet.119.263152
This article has not been copyedited and formatted. The final version may differ from this version.

$R\text{-}_{Vmax}$, $R\text{-}_{CL}$, $R\text{-}_{Content}$ within different levels varied (Fig. 1B, 1C, 1D). One notable example was for the *CYP2A6*4* polymorphism, with $R\text{-}_{Vmax}$ being 39.1% (18.8-100.8%) and 50.0% (25.9-125.0%), $R\text{-}_{CL}$ being 26.7% (2.39-102.9%) and 41.6% (11.1-133.5%), for **1/*1* and **1/*4* genotypes, respectively. For $R\text{-}_{Content}$, the genotype-dependent effect was less obvious.

To obtain more detailed information on how the alteration of CYP2A6 phenotypes among different levels originated, values for MPPGL (microsomal protein per gram of liver), LW/BW (LW, liver weight; BW, body weight) and Q_H (hepatic blood flow) were determined for individuals with *CYP2A6* genetic differences (Fig. 2). Metabolic phenotypes at the liver tissue level ($V_{max\text{-}LT}$, $CL_{\text{-}LT}$) were obtained by multiplying each individual MPPGL by the corresponding individual V_{max} or CL at the microsomal level. LW/BW and Q_H were introduced to determine phenotypes at the organ and organismal level, respectively. However, no significant effect of *CYP2A6* genotype was found.

Genotype-phenotype association

No significant effect of demographic factors, including gender, age, smoking status, drinking habit and medical diagnoses (Supplemental Table 1), on phenotypes was detected (Supplemental Figure 1 ~ 5).

CYP2A6*1B. No significant differences were found for V_{max} and CL at different levels among genetically different individuals with respect to *CYP2A6*1B* polymorphisms. Nor was a significant effect on the K_m value detected. As for the content of CYP2A6 at different levels, the effect varied, with a minor impact on $Content_{\text{-}LT}$ and $Content_{\text{-}L}$, as demonstrated by significantly higher $Content_{\text{-}LT}$ and $Content_{\text{-}L}$ for individuals carrying *CYP2A6*1B/*1B* homozygote as compared to

JPET Fast Forward. Published on December 27, 2019 as DOI: 10.1124/jpet.119.263152
This article has not been copyedited and formatted. The final version may differ from this version.

**1A/*1B* heterozygotes; however, there was no significant difference as compared to wild-type. It is worth mentioning that strongly significant correlations were charted between K_m and V_{max} at different levels among most of the genetic variants, and were dependent upon *CYP2A6* variant. For instance, for V_{max} at microsomal level ($V_{max\text{-}M}$), extremely high correlation was detected with K_m for all *CYP2A6*1B*-related variants (Fig. 3), however, in terms of V_{max} at the isoform level ($V_{max\text{-}P}$), no significant correlation was obtained with K_m for *CYP2A6*1A/*1A* wild-type, and moderate correlation for **1A/*1B* and **1B/*1B* subjects. The mechanism underlying this observation remained to be determined.

CYP2A6*4. *CYP2A6*4* was significantly associated with decreased V_{max} and the effect on phenotype at the cellular level was more markedly significant than that at the molecular level. The $V_{max\text{-}P}$ values of *CYP2A6*1/*4* individuals (15.24 pmol/min/pmol) were dramatically lower than **1/*1* (26.45 pmol/min/pmol) and the $V_{max\text{-}M}$, $V_{max\text{-}LT}$ and $V_{max\text{-}L}$ of *CYP2A6*1/*4* individuals were significantly less than a third of **1/*1* genotypes (Fig. 4). Subjects carrying *CYP2A6*1/*4* genotypes showed lower $content_{\text{-}M}$ (10.62 pmol/mg) and $content_{\text{-}LT}$ (370 pmol/g) when compared with $content_{\text{-}M}$ (18.92 pmol/mg) and $content_{\text{-}LT}$ (629 pmol/g) for subjects with **1/*1*. Observably lower values of $content_{\text{-}M}$ and $content_{\text{-}LT}$ for **1/*4* individuals than those in **1/*1* individuals might explain significantly greater lowered $V_{max\text{-}M}$ and $V_{max\text{-}LT}$ in **1/*4* individuals than **1/*1* subjects. Consistent with this, we found that the $V_{max\text{-}L}$ values of **1/*4* individuals (110.2 nmol/min/kg) were significantly lower than **1/*1* (366.2 nmol/min/kg) individuals.

It should be stated that individuals with the *CYP2A6*1/*4* genotype showed lower K_m than those with the**1/*1* genotype. No statistical difference was found for $CL_{\text{-}P}$, obtained by dividing each individual $V_{max\text{-}P}$ by the individual K_m, between

JPET Fast Forward. Published on December 27, 2019 as DOI: 10.1124/jpet.119.263152
This article has not been copyedited and formatted. The final version may differ from this version.

the**1/*1* (10.76 μl/min/pmol) and **1/*4* (10.83 μl/min/pmol) genotypes, and might be due to the simultaneously lowered $V_{max\text{-}P}$ and K_m in individuals, and effect on $V_{max\text{-}P}$ partially counteracting the negative effect on K_m, as evidenced by significant correlation between K_m and $V_{max\text{-}P}$ ($r=0.457$, $P=2.570\times10^{-5}$) for **1/*1* individuals; however, no such correlation was seen for **1/*4* individuals. The $CL_{\text{-}M}$ (75.05 μl/min/mg), $CL_{\text{-}LT}$ (3.70 ml/min/g) and $CL_{\text{-}L}$ (76.97 ml/min/kg) of CYP2A6 for subjects with **1/*4* was dramatically lower than that for **1/*1* individuals (150.11 μl/min/mg), (6.12 ml/min/g) and (130.12 ml/min/kg), respectively. This could be due to the simultaneously lowered $V_{max\text{-}P}$, $V_{max\text{-}M}$, $V_{max\text{-}LT}$, $V_{max\text{-}L}$ and K_m in individuals, as evidenced by a significant correlation between K_m and V_{max} at different levels, especially for the extremely strong correlation between K_m and $V_{max\text{-}M}$ ($r=0.908$, $P=2.092\times10^{-30}$), K_m and $V_{max\text{-}LT}$ ($r=0.751$, $P=2.285\times10^{-15}$), K_m and $V_{max\text{-}L}$ ($r=0.751$, $P=1.024\times10^{-13}$) for **1/*1* individuals; however, no significant correlation was seen for **1/*4* individuals.

CYP2A6*9. Consistent with *CYP2A6*1B*, the effect of *CYP2A6*9* on phenotypes was not as significant as with *CYP2A6*4* (Fig. 5). Only subjects with *CYP2A6*1/*1* wild-type and **1/*9* heterozygotes were taken into analysis, without considering **9/*9* homozygotes since only three individuals carried the **9/*9* genotype. No significant difference was found in $V_{max\text{-}P}$ for **1/*1* carriers as compared to **1/*9* carriers, and dramatically a lower K_m for individuals with **1/*9* (2.07 μM) than for**1/*1* (3.03 μM) genotypes. The $CL_{\text{-}P}$ values, acquired by dividing individual $V_{max\text{-}P}$ by each K_m as described above, of **1/*9* (12.72 μl/min/pmol) individuals seemed to be higher than**1/*1* (8.71 μl/min/pmol) subjects; however, this difference was not statistically significant. For both $V_{max\text{-}M}$ and $V_{max\text{-}LT}$, **1/*9* was associated with decreased activity as compared to wild-type, which might be related to

JPET Fast Forward. Published on December 27, 2019 as DOI: 10.1124/jpet.119.263152
This article has not been copyedited and formatted. The final version may differ from this version.

seemingly lower $Content_{-M}$ and $Content_{-LT}$ for **1/*9* individuals, in spite of lack of statistical difference. Moreover, the CL_{-M} for *2A6*1/*9* was significantly lower than that of **1/*1* individuals, which might be due to simultaneously lowered V_{max-M} and $Content_{-M}$ and a strongly significant association between K_m and V_{max-M}. For V_{max-L}, $Content_{-LT}$, $Content_{-L}$, CL_{-LT} and CL_{-L}, no significant alteration was related with **9* polymorphisms, even with a lower tendency of V_{max-L}, $Content_{-LT}$ and $Content_{-L}$ for **1/*9* individuals. We note that K_m was strongly positively associated with V_{max} within different levels for both *CYP2A6*1/*1* and *CYP2A6*1/*9* genotypes except for V_{max-P} in *CYP2A6*9* wild-type carriers.

Inter-genotype variation

Inter-genotype individual variations of CYP2A6 phenotypes at different levels were charted and significant differences in variability among genetically different individuals are presented as seen in Fig. 6. Generally speaking, the *CYP2A6*4* polymorphism led to the most remarkable alteration with decreased V_{max}, Content and CL at the majority of levels, while *CYP2A6*1B* and **9* led to less obvious alteration either with increased or decreased phenotypes at some levels. Compared with wild-type, various phenotypes such as V_{max-P}, V_{max-M}, V_{max-LT}, V_{max-L}, $Content_{-M}$, $Content_{-LT}$, CL_{-M}, CL_{-LT}, CL_{-L} and CL_{-H} of **1/*4* showed an approximate decrease of 51%, 85%, 80%, 88%, 51%, 51%, 71%, 59%, 62% and 57%, respectively, while the $Content_{-L}$ and CL_{-P} were basically unchanged. For *CYP2A6*1B*, $Content_{-LT}$, $Content_{-L}$, CL_{-LT}, CL_{-L} and CL_{-H} of mutant homozygotes was significantly higher than that of heterozygotes, while heterozygotes and mutant homozygotes were basically unchanged when compared with wild-type. Most notably, *CYP2A6*1B* led to distinctly increased $Content_{-L}$ with heterozygotes and mutant homozygotes showing 2.80-fold and 6.87-fold increases as compared with wild-type, respectively. However,

JPET Fast Forward. Published on December 27, 2019 as DOI: 10.1124/jpet.119.263152
This article has not been copyedited and formatted. The final version may differ from this version.

CL_{-L} did not confirm this trend of change. With regard to *CYP2A6*9*, lowered V_{max-P}, V_{max-M}, V_{max-LT}, $Content_{-L}$, CL_{-L} of mutant heterozygotes was detected when compared with wild-type, while $Content_{-M}$, CL_{-P} and CL_{-M} showed a reverse trend.

Moreover, with regard to K_m, in line with other phenotypes, the most remarkable alteration was with **1/*4* genotypes, with about a 49% reduction. While *9 polymorphisms led to distinctly lower K_m, with heterozygotes and mutant homozygotes showing 32% and 47% decreases as compared with wild-type, respectively. For *CYP2A6*1B*, K_m of **1B* carriers was basically unchanged for heterozygotes and homozygotes.

Discussion

In this present study of 90 human liver samples, the systematic delineation of a *CYP2A6* genotype-phenotype model including protein content and metabolic activity of CYP2A6 at various levels such as molecular, cellular (microsomal, tissue, organ), and organismal levels was generated. We determined the median and range for the protein content, V_{max}, and CL as well as relative phenotypes ($R_{-Content}$, R_{-Vmax}, and R_{-CL}) at each level with every *CYP2A6* genotype to elucidate how different *CYP2A6* genotypes yield phenotypic traits (protein content and enzyme activity) at different levels. The high relative intra-individual percentage coefficients of variation (ICVs) of phenotypes indicates large intra-individual variation within different levels, sometimes in a genotype-dependent manner. Inter-genotype analysis indicated that *CYP2A6*4* had the most obvious effect on phenotypes, and protein content might be related to the *CYP2A6*4* allele. The correlation of phenotypes from the molecular level to the cellular level, and then to the organismal level demonstrates how genotypes may affect phenotypes and could be considered for better understanding of

JPET Fast Forward. Published on December 27, 2019 as DOI: 10.1124/jpet.119.263152
This article has not been copyedited and formatted. The final version may differ from this version.

phenotypic variation and assessment of phenotypic outcome with specific genotypes.

We did find that the alteration of phenotypes from the molecular level to the cellular level, and then to organismal level varied greatly, which agrees with our previous studies (Zhang et al., 2015b; Gao et al., 2017a). However, our previous study on the *CYP2D6* genotype-phenotype association (Gao et al., 2017a) indicated the effect of the *CYP2D6* genotype on the metabolic phenotype at each level, but did not consider the alteration of phenotypes among different levels. In this study, the ICVs of $R\text{-}_{Vmax}$, $R\text{-}_{CL}$, $R\text{-}_{Content}$ within different levels indicated noticeable intra-individual variation and varied with the *CYP2A6* genotype. Take the *CYP2A6*4* allele for example; the ICVs of $R\text{-}_{CL}$ for *CYP2A6*1/*4*, 41.6% (11.1-133.5%) was nearly 1.56-fold of that for the **1/*1* genotype, 26.7% (2.39-102.9%). While for $R\text{-}_{Vmax}$, the difference was 1.28-fold. The reason for these differences might be the superimposed effect of genotype on phenotype, since the effect on the molecular level might influence the cellular level, and then to the organismal level. In line with this speculation, the effect on CL might be the combined effect on V_{max} and K_m, since CL was obtained by dividing V_{max} by K_m. However, the precise mechanism underlying this needs further exploration.

The most impactful genotype on phenotype-effect was with *CYP2A6*4*, which is a gene deletion genotype, in contrast to the *1B genotype (located in 3' untranslated region) and the *9 (mutation located in the 'TATA box') being the least impactful phenotype as measured herein. Results are in agreement with a series of previous studies (Ujjin et al., 2002; Yoshida et al., 2003; Wang et al., 2006; Wang et al., 2011; Tanner et al., 2017), though those studies were conducted either *in vitro* by site-directed mutagenesis or *in vivo* by phenotyping using substrates. The location and type of mutation is clearly important when evaluating the phenotypic impact of

different genotypes.

It is noteworthy that protein content might play an important role for extrapolation from the genotype of *CYP2A6* to the different levels of phenotypes, especially for *CYP2A6*4*. *CYP2A6*4*, a coding deletion genotype, was associated with significant decreased protein and acitvity in our study and also with the same effect in previous reports (Peamkrasatam et al., 2006; Wang et al., 2011). However, on such trend was detected in one study demonstrating protein content correlated well with activity (Tanner et al., 2017). The reason for the inconsistencies might be that liver samples conducted in that study were from two liver banks with different ethnicities and only one *CYP2A6*1/*4* sample was identified, so the effect of the *CYP2A6*4* genotype on phenotype could not be well evaluated. Our study focused on known but less common polymorphisms that were present at higher levels in the Chinese population. As depicted in Fig. 4, the markedly lower $Content_{-M}$ (10.62 pmol/mg) and $Content_{-LT}$ (3.70 ml/min/g) in **1/*4* genotypes might help explain the much greater decrease in V_{max-M}, V_{max-LT} and V_{max-L} than V_{max-P} correlated with *CYP2A6*4*. This was consistent with the view that protein content and activity might play a role in determining metabolic phenotypes and susceptible to disease (Tian et al., 2016; Gao et al., 2018a; Gao et al., 2018b; Gao et al., 2018c).

Most notably, one interesting finding was the highly significant positive correlation between K_m and V_{max} at each level in the**1/*1* wild-type. Given that, we speculate that the significantly lowered CL_{-M}, CL_{-LT}, CL_{-L} in **4* carriers might be due to the more prominent decreased V_{max} than K_m at each corresponding level. While for the phenotype at the molecular level, the almost uniform extent of change for V_{max-P} and K_m might be the reason for the insignificant alteration of CL_{-P} related to the **4* variation. But the explicit mechanism underlying this remains unknown and needs

further investigation.

The inter-individual variation of CYP2A6 phenotypes in relation to different genotypes at various levels may play a role in interethnic or inter-individual variability for CYP2A6 phenotypes and the risk for CYP2A6-related disease. *CYP2A6*4*, in particular, correlated with lower 2A6 phenotypes at a number of levels. For example, the median value of $V_{max\text{-}M}$, $Content_{\text{-}M}$, and $CL_{\text{-}M}$ was decreased to 15%, 49%, 29%, respectively, in **4* carriers when compared with *1 wild-type carriers. This likely contributes to the known slower cotinine metabolism in Chinese-Americans than Caucasians (Benowitz et al., 2002), since the frequency of *CYP2A6*4* in Chinese was 6.6~15.1%, much higher than the Caucasian level of 0.5~4.9% (Xu et al., 2002).

The inter-ethnic as well as inter-individual variation in metabolic phenotypes might have several important clinical implications; for instance, CYP2A6-related metabolic activity (e.g nicotine metabolism), behaviors (Malaiyandi et al., 2006) (i.e. smoking) and disease (Fujieda et al., 2004) (i.e. lung cancer). Genetic studies on *CYP2A6* in Japanese indicated a decreased rate of lung cancer in inactive *CYP2A6* variants carriers in comparison with wild-type (Miyamoto et al., 1999). In addition to the cigarette smoking-related lung cancer, CYP2A6 is also involved in the metabolism of many other procarcinogens. However, a clearer understanding of the role for genotypes of *CYP2A6* in relation to disease is needed before conclusions can be reached.

Since liver samples of perfectly healthy persons with comprehensive background information are difficult to obtain, the liver samples used here were from patients undergoing hepatic surgery. However, the donors were with clear medical diagnoses

mostly of cavernous hemangioma of liver, and mitigated by techniques and confirmed by analysis (Supplemental Figure 5) to minimize impact of tumors and other demographic factors (Supplemental Figure 1~4). Moreover, a total of 90 samples studied here with comprehensive background information is a large number of human samplings and is certainly adequate. Even so, high variability existed along with relatively low numbers per grouping, and might still affect the ability to differentiate smaller differences. Many more samples are needed to rule out idiosyncratic variation as much as possible. Since it was not easy to simultaneously obtain *in vivo* and *in vitro* results for the same cohort of samples, no actual *in vivo* measurements were made in our study. We utilized *in vitro* measurements at different levels to predict hepatic clearance by *in vitro-in vivo* extrapolation to the *in vivo* level. After correction, our *in vivo* extrapolation by calculation yielded high accuracy, as indicated by the predicted CL of CYP2A6 matching 82.8% of the cases within 2-fold error when compared with actual observed $CL_{in\ vivo}$ determined in other studies (Ritschel et al., 1977; Gao et al., 2016). Even so, actual *in vivo* measurements are additional efforts needed to draw more clear and convincing conclusions.

In conclusion, we have developed a comprehensive *CYP2A6* genotype-to-phenotype model. In this model a role for the *CYP2A6* genotypes in influencing phenotypic variation at various levels was evaluated, although clearly may not be sufficient to explain variation in all phenotypic outcomes. It does provide the basal data for CYP2A6 content and metabolic activities at different levels with each *CYP2A6* genotype, as well as fundamental hierarchical relationships between *CYP2A6* genotypes and phenotypes. We identified a key role for decreased protein content for the *CYP2A6*4* genotype that is related to decreased metabolic phenotypes. These findings might help open new approaches for considering how genetic variation

is translated to the phenotype of individuals, which might be a further step on the way to making useful predictions of outcomes for a particular individual as a part of personalized medicine and disease risk.

Acknowledgement

The authors would like to thank professor Song-He Shi and Xue-Zhong Shi for their valuable suggestions during the statistical analysis of data for this manuscript.

Author Contributions

Participated in research design: Qiao.

Conducted experiments: Fang, Wang.

Contributed new reagents or analytic tools: Guo, Zhang, Wen.

Performed data analysis: Fang, Wang.

Wrote or contributed to the writing of the manuscript: Fang, Qiao, Gao, Xing.

JPET Fast Forward. Published on December 27, 2019 as DOI: 10.1124/jpet.119.263152
This article has not been copyedited and formatted. The final version may differ from this version.

References

Barter ZE, Tucker GT and Rowland-Yeo K (2013) Differences in cytochrome p450-mediated pharmacokinetics between chinese and caucasian populations predicted by mechanistic physiologically based pharmacokinetic modelling. *Clinical pharmacokinetics* **52**:1085-1100.

Benowitz NL, Perez-Stable EJ, Herrera B and Jacob P, 3rd (2002) Slower metabolism and reduced intake of nicotine from cigarette smoking in Chinese-Americans. *Journal of the National Cancer Institute* **94**:108-115.

Bradford MM (1976) A rapid and sensitive method for the quantitation of microgram quantities of protein utilizing the principle of protein-dye binding. *Analytical biochemistry* **72**:248-254.

Dai DP, Xu RA, Hu LM, Wang SH, Geng PW, Yang JF, Yang LP, Qian JC, Wang ZS, Zhu GH, Zhang XH, Ge RS, Hu GX and Cai JP (2014) CYP2C9 polymorphism analysis in Han Chinese populations: building the largest allele frequency database. *The pharmacogenomics journal* **14**:85-92.

Fang Y, Gao J, Wang T, Tian X, Gao N, Zhou J, Zhang HF, Wen Q, Jin H, Xing YR and Qiao HL (2018a) Intraindividual Variation and Correlation of Cytochrome P450 Activities in Human Liver Microsomes. *Molecular pharmaceutics* **15**:5312-5318.

Fang Y, Gao N, Tian X, Zhou J, Zhang HF, Gao J, He XP, Wen Q, Jia LJ, Jin H and Qiao HL (2018b) Effect of P450 Oxidoreductase Polymorphisms on the Metabolic Activities of Ten Cytochrome P450s Varied by Polymorphic CYP Genotypes in Human Liver Microsomes. *Cellular physiology and biochemistry : international journal of experimental cellular physiology, biochemistry, and pharmacology* **47**:1604-1616.

Fujieda M, Yamazaki H, Saito T, Kiyotani K, Gyamfi MA, Sakurai M, Dosaka-Akita H, Sawamura Y, Yokota J, Kunitoh H and Kamataki T (2004) Evaluation of CYP2A6 genetic polymorphisms as determinants of smoking behavior and tobacco-related lung cancer risk in male Japanese smokers. *Carcinogenesis* **25**:2451-2458.

Fukami T, Nakajima M, Higashi E, Yamanaka H, Sakai H, McLeod HL and Yokoi T (2005) Characterization of novel CYP2A6 polymorphic alleles (CYP2A6*18 and CYP2A6*19) that

affect enzymatic activity. Drug Metab Dispos 33: 1202-1210.

Gao J, Tian X, Zhou J, Cui MZ, Zhang HF, Gao N, Wen Q and Qiao HL (2017a) From Genotype to Phenotype: Cytochrome P450 2D6-Mediated Drug Clearance in Humans. *Molecular pharmaceutics* **14**:649-657.

Gao J, Wang GJ, Wang Z, Gao N, Li J, Zhang YF, Zhou J, Zhang HX, Wen Q, Jin H and Qiao HL (2017b) High CYP2E1 activity correlates with hepatofibrogenesis induced by nitrosamines. *Oncotarget* **8**:112199-112210.

Gao J, Wang J, Gao N, Tian X, Zhou J, Fang Y, Zhang HF, Wen Q, Jia LJ, Zou D and Qiao HL (2017c) Prediction of cytochrome P450-mediated drug clearance in humans based on the measured activities of selected CYPs. *Bioscience reports* **37**.

Gao J, Wang Z, Wang GJ, Gao N, Li J, Zhang YF, Zhou J, Zhang HX, Wen Q, Jin H and Qiao HL (2018a) From hepatofibrosis to hepatocarcinogenesis: Higher cytochrome P450 2E1 activity is a potential risk factor. *Molecular carcinogenesis* **57**:1371-1382.

Gao J, Wang Z, Wang GJ, Zhang HX, Gao N, Wang J, Wang CE, Chang Z, Fang Y, Zhang YF, Zhou J, Jin H and Qiao HL (2018b) Higher CYP2E1 Activity Correlates with Hepatocarcinogenesis Induced by Diethylnitrosamine. *The Journal of pharmacology and experimental therapeutics* **365**:398-407.

Gao J, Zhou J, He XP, Zhang YF, Gao N, Tian X, Fang Y, Wen Q, Jia LJ, Jin H and Qiao HL (2016a) Changes in cytochrome P450s-mediated drug clearance in patients with hepatocellular carcinoma in vitro and in vivo: a bottom-up approach. *Oncotarget* **7**:28612-28623.

Gao N, Li J, Li MR, Qi B, Wang Z, Wang GJ, Gao J and Qiao HL (2018c) Higher activity of alcohol dehydrogenase is correlated with hepatic fibrogenesis. *The Journal of pharmacology and experimental therapeutics*.

Gao N, Tian X, Fang Y, Zhou J, Zhang H, Wen Q, Jia L, Gao J, Sun B, Wei J, Zhang Y, Cui M and Qiao H (2016b) Gene polymorphisms and contents of cytochrome P450s have only limited effects on metabolic activities in human liver microsomes. *Eur J Pharm Sci* **92**:86-97.

Li J, Zhou L, Wang H, Yan H, Li N, Zhai R, Jiao F, Hao F, Jin Z, Tian F, Peng B, Zhang Y and Qian X

(2015) A new sample preparation method for the absolute quantitation of a target proteome using (18)O labeling combined with multiple reaction monitoring mass spectrometry. *The Analyst* **140**:1281-1290.

Malaiyandi V, Lerman C, Benowitz NL, Jepson C, Patterson F and Tyndale RF (2006) Impact of CYP2A6 genotype on pretreatment smoking behaviour and nicotine levels from and usage of nicotine replacement therapy. *Molecular psychiatry* **11**:400-409.

Mega JL, Close SL, Wiviott SD, Shen L, Hockett RD, Brandt JT, Walker JR, Antman EM, Macias W, Braunwald E and Sabatine MS (2009) Cytochrome p-450 polymorphisms and response to clopidogrel. *The New England journal of medicine* **360**:354-362.

Miyamoto M, Umetsu Y, Dosaka-Akita H, Sawamura Y, Yokota J, Kunitoh H, Nemoto N, Sato K, Ariyoshi N and Kamataki T (1999) CYP2A6 gene deletion reduces susceptibility to lung cancer. *Biochemical and biophysical research communications* **261**:658-660.

Murdter TE, Kerb R, Turpeinen M, Schroth W, Ganchev B, Bohmer GM, Igel S, Schaeffeler E, Zanger U, Brauch H and Schwab M (2012) Genetic polymorphism of cytochrome P450 2D6 determines oestrogen receptor activity of the major infertility drug clomiphene via its active metabolites. *Human molecular genetics* **21**:1145-1154.

Oscarson M, McLellan RA, Gullsten H, Yue QY, Lang MA, Bernal ML, Sinues B, Hirvonen A, Raunio H, Pelkonen O and Ingelman-Sundberg M (1999) Characterisation and PCR-based detection of a CYP2A6 gene deletion found at a high frequency in a Chinese population. *FEBS letters* **448**:105-110.

Palma BB, Silva ESM, Vosmeer CR, Lastdrager J, Rueff J, Vermeulen NP and Kranendonk M (2010) Functional characterization of eight human cytochrome P450 1A2 gene variants by recombinant protein expression. *The pharmacogenomics journal* **10**:478-488.

Peamkrasatam S, Sriwatanakul K, Kiyotani K, Fujieda M, Yamazaki H, Kamataki T and Yoovathaworn K (2006) In vivo evaluation of coumarin and nicotine as probe drugs to predict the metabolic capacity of CYP2A6 due to genetic polymorphism in Thais. *Drug metabolism and pharmacokinetics* **21**:475-484.

Ritschel WA, Brady ME, Tan HS, Hoffmann KA, Yiu IM and Grummich KW (1977) Pharmacokinetics of coumarin and its 7-hydroxy-metabolites upon intravenous and peroral administration of coumarin in man. Eur J Clin Pharmacol 12: 457-461.

Sadeque AJ, Fisher MB, Korzekwa KR, Gonzalez FJ and Rettie AE (1997) Human CYP2C9 and CYP2A6 mediate formation of the hepatotoxin 4-ene-valproic acid. *The Journal of pharmacology and experimental therapeutics* **283**:698-703.

Shuker N, Bouamar R, van Schaik RH, Clahsen-van Groningen MC, Damman J, Baan CC, van de Wetering J, Rowshani AT, Weimar W, van Gelder T and Hesselink DA (2016) A Randomized Controlled Trial Comparing the Efficacy of Cyp3a5 Genotype-Based With Body-Weight-Based Tacrolimus Dosing After Living Donor Kidney Transplantation. *American journal of transplantation : official journal of the American Society of Transplantation and the American Society of Transplant Surgeons* **16**:2085-2096.

Tanner JA, Prasad B, Claw KG, Stapleton P, Chaudhry A, Schuetz EG, Thummel KE and Tyndale RF (2017) Predictors of Variation in CYP2A6 mRNA, Protein, and Enzyme Activity in a Human Liver Bank: Influence of Genetic and Nongenetic Factors. J Pharmacol Exp Ther 360: 129-139.

Tennessen JA, Bigham AW, O'Connor TD, Fu W, Kenny EE, Gravel S, McGee S, Do R, Liu X, Jun G, Kang HM, Jordan D, Leal SM, Gabriel S, Rieder MJ, Abecasis G, Altshuler D, Nickerson DA, Boerwinkle E, Sunyaev S, Bustamante CD, Bamshad MJ, Akey JM, Broad GO, Seattle GO and Project NES (2012) Evolution and functional impact of rare coding variation from deep sequencing of human exomes. *Science* **337**:64-69.

Tian X, Li HM, Wei JY, Liu BJ, Zhang YH, Wang GJ, Chang JB and Qiao HL (2016) Preclinical Pharmacokinetics, Tissue Distribution, and Plasma Protein Binding of Sodium (+/-)-5-Bromo-2-(alpha-Hydroxypentyl) Benzoate (BZP), an Innovative Potent Anti-ischemic Stroke Agent. *Front Pharmacol* **7**:255.

Ujjin P, Satarug S, Vanavanitkun Y, Daigo S, Ariyoshi N, Yamazaki H, Reilly PE, Moore MR and Kamataki T (2002) Variation in coumarin 7-hydroxylase activity associated with genetic polymorphism of cytochrome P450 2A6 and the body status of iron stores in adult Thai males

and females. *Pharmacogenetics* **12**:241-249.

Wang H, Bian T, Liu D, Jin T, Chen Y, Lin A and Chen C (2011) Association analysis of CYP2A6 genotypes and haplotypes with 5-fluorouracil formation from tegafur in human liver microsomes. *Pharmacogenomics* **12**:481-492.

Wang J, Pitarque M and Ingelman-Sundberg M (2006) 3'-UTR polymorphism in the human CYP2A6 gene affects mRNA stability and enzyme expression. *Biochemical and biophysical research communications* **340**:491-497.

Wang XF, Li B, Lan X, Yuan D, Zhang M, Wei YG, Zeng Y, Wen TF, Zhao JC and Yan LN (2008) [Establishment of formula predicting adult standard liver volume for liver transplantation]. *Zhonghua wai ke za zhi [Chinese journal of surgery]* **46**:1129-1132.

Werk AN and Cascorbi I (2014) Functional gene variants of CYP3A4. *Clinical pharmacology and therapeutics* **96**:340-348.

White IN, Razvi N, Gibbs AH, Davies AM, Manno M, Zaccaro C, De Matteis F, Pahler A and Dekant W (2001) Neoantigen formation and clastogenic action of HCFC-123 and perchloroethylene in human MCL-5 cells. *Toxicology letters* **124**:129-138.

Xu C, Goodz S, Sellers EM and Tyndale RF (2002) CYP2A6 genetic variation and potential consequences. *Advanced drug delivery reviews* **54**:1245-1256.

Yoshida R, Nakajima M, Nishimura K, Tokudome S, Kwon JT and Yokoi T (2003) Effects of polymorphism in promoter region of human CYP2A6 gene (CYP2A6*9) on expression level of messenger ribonucleic acid and enzymatic activity in vivo and in vitro. *Clinical pharmacology and therapeutics* **74**:69-76.

Yuan D, Lu T, Wei YG, Li B, Yan LN, Zeng Y, Wen TF and Zhao JC (2008) Estimation of standard liver volume for liver transplantation in the Chinese population. *Transplantation proceedings* **40**:3536-3540.

Zanger UM and Schwab M (2013) Cytochrome P450 enzymes in drug metabolism: regulation of gene expression, enzyme activities, and impact of genetic variation. *Pharmacology & therapeutics* **138**:103-141.

Zhang H, Gao N, Liu T, Fang Y, Qi B, Wen Q, Zhou J, Jia L and Qiao H (2015a) Effect of Cytochrome b5 Content on the Activity of Polymorphic CYP1A2, 2B6, and 2E1 in Human Liver Microsomes. *PloS one* **10**:e0128547.

Zhang H, Gao N, Tian X, Liu T, Fang Y, Zhou J, Wen Q, Xu B, Qi B, Gao J, Li H, Jia L and Qiao H (2015b) Content and activity of human liver microsomal protein and prediction of individual hepatic clearance in vivo. *Scientific reports* **5**:17671.

Zhang HF, Wang HH, Gao N, Wei JY, Tian X, Zhao Y, Fang Y, Zhou J, Wen Q, Gao J, Zhang YJ, Qian XH and Qiao HL (2016) Physiological Content and Intrinsic Activities of 10 Cytochrome P450 Isoforms in Human Normal Liver Microsomes. *J Pharmacol Exp Ther* **358**:83-93.

Zhou J, Wen Q, Li SF, Zhang YF, Gao N, Tian X, Fang Y, Gao J, Cui MZ, He XP, Jia LJ, Jin H and Qiao HL (2016) Significant change of cytochrome P450s activities in patients with hepatocellular carcinoma. *Oncotarget* **7**:50612-50623.

Zhu HJ, Yuan SH, Fang Y, Sun XZ, Kong H and Ge WH (2011) The effect of CYP3A5 polymorphism on dose-adjusted cyclosporine concentration in renal transplant recipients: a meta-analysis. *The pharmacogenomics journal* **11**:237-246.

Zordoky BN and El-Kadi AO (2010) Effect of cytochrome P450 polymorphism on arachidonic acid metabolism and their impact on cardiovascular diseases. *Pharmacology & therapeutics* **125**:446-463.

Footnotes

This work was supported by the National Natural Science Foundation of China (No. 81473279, No.81673507, No.8187 2931 and U1804169).

JPET Fast Forward. Published on December 27, 2019 as DOI: 10.1124/jpet.119.263152
This article has not been copyedited and formatted. The final version may differ from this version.

Figure legends

Figure 1. ICV of relative V_{max}, CL and Content of CYP2A6 at different levels (n=90). ICV of relative V_{max}, CL and Content of CYP2A6 for total samples (A) and ICV of relative V_{max} (B), CL (C) and Content (D) sorted by different *CYP2A6* genotypes. ICV, intraindividual percentage coefficient of variation, was calculated as the standard deviation of relative V_{max}, CL and Content divided by the corresponding average value for that case. Each level's relative V_{max}, CL and Content was calculated as the individual V_{max}, CL and Content divided by the median for that level. Horizontal lines represent medians with the interquartile range. (**1A/*1A*, n=11; **1A/*1B*, n=51; **1B/*1B*, n=16. **1/*1*, n=78; **1*4*, n=12.**1/*1*, n=46; **1/*9*, n=29; **9/*9*, n=3).

Figure 2. Effect of *CYP2A6* genotypes on MPPGL (A), LW/BW (B) and Q_H (C). MPPGL, microsomal protein per gram of liver. LW: liver weight. BW: body weight. QH: hepatic blood flow. Horizontal lines represent medians with the interquartile range. (**1A/*1A*, n=11; **1A/*1B*, n=51; **1B/*1B*, n=16.**1/*1*, n=78; **1*4*, n=12. **1/*1*, n=46; **1/*9*, n=29; **9/*9*, n=3).

Figure 3. Genotype-phenotype associations varied by *CYP2A6*1B* polymorphisms. $V_{max\text{-}P}$, $V_{max\text{-}M}$, $V_{max\text{-}LT}$, $V_{max\text{-}L}$, $Content_{\text{-}M}$, $Content_{\text{-}LT}$, $Content_{\text{-}L}$, $CL_{\text{-}P}$, $CL_{\text{-}M}$, $CL_{\text{-}LT}$, $CL_{\text{-}L}$, $CL_{\text{-}H}$ were divided by **1A/*1A*, **1A/*1B* and **1B/*1B* genotypes (**1A/*1A*, n=11; **1A/*1B*, n=51; **1B/*1B*, n=16). $V_{max\text{-}P}$ (pmol/min/pmol), $CL_{\text{-}P}$ (μl/min/pmol), the molecular phenotype or phenotype at the protein level. $V_{max\text{-}M}$ (pmol/min/mg), $CL_{\text{-}M}$ (μl/min/mg), $Content_{\text{-}M}$ (pmol/mg), the sub-cellular phenotype or phenotype at microsomal level. $V_{max\text{-}LT}$ (nmol/min/g), $CL_{\text{-}LT}$ (ml/min/g), $Content_{\text{-}LT}$ (pmol/g),

JPET Fast Forward. Published on December 27, 2019 as DOI: 10.1124/jpet.119.263152
This article has not been copyedited and formatted. The final version may differ from this version.

the tissue phenotype or phenotype at liver tissue level. $V_{max\text{-}L}$ (μmol/min/kg), $CL_{\text{-}L}$ (ml/min/kg), $Content_{\text{-}L}$ (pmol/kg), the organ phenotype or phenotype at liver level. K_m (μM), the Michaelis–Menten constant.

Figure 4. Genotype-phenotype associations varied by *CYP2A6*4* polymorphisms. $V_{max\text{-}P}$, $V_{max\text{-}M}$, $V_{max\text{-}LT}$, $V_{max\text{-}L}$, $Content_{\text{-}M}$, $Content_{\text{-}LT}$, $Content_{\text{-}L}$, $CL_{\text{-}P}$, $CL_{\text{-}M}$, $CL_{\text{-}LT}$, $CL_{\text{-}L}$ were divided by **1/*1*, **1/*4* genotypes (**1/*1*, n=78; **1*4*, n=12). $V_{max\text{-}P}$ (pmol/min/pmol), $CL_{\text{-}P}$ (μl/min/pmol), the molecular phenotype or phenotype at the protein level. $V_{max\text{-}M}$ (pmol/min/mg), $CL_{\text{-}M}$ (μl/min/mg), $Content_{\text{-}M}$ (pmol/mg), the sub-cellular phenotype or phenotype at microsomal level. $V_{max\text{-}LT}$ (nmol/min/g), $CL_{\text{-}LT}$ (ml/min/g), $Content_{\text{-}LT}$ (pmol/g), the tissue phenotype or phenotype at liver tissue level. $V_{max\text{-}L}$ (μmol/min/kg), $CL_{\text{-}L}$ (ml/min/kg), $Content_{\text{-}L}$ (pmol/kg), the organ phenotype or phenotype at liver level. K_m (μM), the Michaelis–Menten constant.

Figure 5. Genotype-phenotype associations varied by *CYP2A6*9* polymorphisms. $V_{max\text{-}P}$, $V_{max\text{-}M}$, $V_{max\text{-}LT}$, $V_{max\text{-}L}$, $Content_{\text{-}M}$, $Content_{\text{-}LT}$, $Content_{\text{-}L}$, $CL_{\text{-}P}$, $CL_{\text{-}M}$, $CL_{\text{-}LT}$, $CL_{\text{-}L}$ were divided by **1/*1*, **1/*9*, **9/*9* genotypes (**1/*1*, n=46; **1/*9*, n=29; **9/*9*, n=3). $V_{max\text{-}P}$ (pmol/min/pmol), $CL_{\text{-}P}$ (μl/min/pmol), the molecular phenotype or phenotype at the protein level. $V_{max\text{-}M}$ (pmol/min/mg), $CL_{\text{-}M}$ (μl/min/mg), $Content_{\text{-}M}$ (pmol/mg), the sub-cellular phenotype or phenotype at microsomal level. $V_{max\text{-}LT}$ (nmol/min/g), $CL_{\text{-}LT}$ (ml/min/g), $Content_{\text{-}LT}$ (pmol/g), the tissue phenotype or phenotype at the liver tissue level. $V_{max\text{-}L}$ (μmol/min/kg), $CL_{\text{-}L}$ (ml/min/kg), $Content_{\text{-}L}$ (pmol/kg), the organ phenotype or phenotype at liver level. K_m (μM), the Michaelis – Menten constant.

JPET Fast Forward. Published on December 27, 2019 as DOI: 10.1124/jpet.119.263152
This article has not been copyedited and formatted. The final version may differ from this version.

Figure 6. The diversity in CYP2A6 phenotypes at different levels. $V_{max\text{-}P}$, $V_{max\text{-}M}$, $V_{max\text{-}LT}$, $V_{max\text{-}L}$, $Content_{\text{-}M}$, $Content_{\text{-}LT}$, $Content_{\text{-}L}$, $CL_{\text{-}P}$, $CL_{\text{-}M}$, $CL_{\text{-}LT}$, $CL_{\text{-}L}$, $CL_{\text{-}H}$, K_m were sorted by different *CYP2A6* genotypes. As compared with wild-type, fold-changes of other genotypes were calculated by dividing the absolute value of the median for the phenotype by the absolute value of median for the corresponding wild-type. The fold-change for all phenotypes with wild-type were defined as one. [*CYP2A6*1B* (**1A/*1A*, n=11; **1A/*1B*, n=51; **1B/*1B*, n=16); *CYP2A6*4* (**1/*1*, n=78; **1*4*, n=12); *CYP2A6*9* (**1/*1*, n=46; **1/*9*, n=29; **9/*9*, n=3). $^{*}P<0.05$, $^{**}P<0.01$, $^{***}P<0.001$ *vs* wild type; $^{\#}P<0.05$, $^{\#\#}P<0.01$ *vs* mutant heterozygotes.

JPET Fast Forward. Published on December 27, 2019 as DOI: 10.1124/jpet.119.263152
This article has not been copyedited and formatted. The final version may differ from this version.

Tables

Table 1. Definitions of phenotypes for CYP2A6 at different levels

Level	V_{max}		CL_{int}		Content	
	def	units	def	units	def	units
Molecular (Protein)	$V_{max\text{-}P}$	mol/min/pmol	$CL_{\text{-}P}$	µl/min/pmol	——	——
Sub-cellular (Microsomal)	$V_{max\text{-}M}$	mol/min/mg	$CL_{\text{-}M}$	µl/min/mg	$Content_{\text{-}M}$	pmol/mg
Tissue (Liver tissue)	$V_{max\text{-}LT}$	mol/min/g	$CL_{\text{-}LT}$	µl/min/g	$Content_{\text{-}LT}$	pmol/g
Organ (Liver)	$V_{max\text{-}L}$	mol/min/kg	$CL_{\text{-}L}$	µl/min/kg	$Content_{\text{-}L}$	nmol/kg
Organism (*In Vivo*)	——	——	$CL_{\text{-}H}$	ml/min	——	——

def, definitons.

Molecular level, or phenotype at the protein level, $V_{max\text{-}P}$ (pmol/min/pmol), $CL_{\text{-}P}$ (µl/min/pmol).

Sub-cellular level, or phenotype at microsomal level, $V_{max\text{-}M}$ (pmol/min/mg), $CL_{\text{-}M}$ (µl/min/mg), $Content_{\text{-}M}$ (pmol/mg).

Tissue level, or phenotype at liver tissue level, $V_{max\text{-}LT}$ (pmol/min/g), $CL_{\text{-}LT}$ (µl/min/g), $Content_{\text{-}LT}$ (pmol/g).

Organ level, or phenotype at liver level, $V_{max\text{-}L}$(nmol/min/kg), $CL_{\text{-}L}$ (µl/min/kg), $Content_{\text{-}L}$ (nmol/kg).

Organism level, or phenotype (clearance) at *in vivo* level, $CL_{\text{-}H}$ (ml/min).

Table 2. CYP2A6 phenotypes at different levels (n=90)

Level		V_{max}			CL			Content		
		Range	Ratio	R_{-Vmax}	Range	Ratio	R_{-CL}	Range	Ratio	$R_{-Content}$
Molecular	M	19.79			8.73			-----		
			63.8	1.16±0.71		52.9	1.19±0.86		-----	-----
(Protein)	R	1.08-68.89			0.83-43.89			-----		
Sub-cellular	M	354.4			144.8			14.60		
			151	1.07±0.78		454	0.97±0.43		38.1	1.22±0.75
(Microsomal)	R	9.47-1430			1.20-544.7			1.44-54.89		
Tissue	M	12.27			5.19			637.6		
			247	1.28±1.14		284	1.12±0.68		42.6	1.09±0.56
(Liver tissue)	R	0.25-61.74			0.06-17.03			71.17-3031		
Organ	M	267			109.2			893.2		
			214	2.08±1.86[abc]		273	1.13±0.70		94.1	1.14±0.89
(Liver)	R	6.22-1337			1.36-371.2			58.43-5497		

Organism	M	-----			287.3			-----				
			-----	-----		169	1.05±0.48		-----	-----		
(*In Vivo*)	R	-----			3.87-653.5			-----				

M, median; R, range. Relative phenotypes, $R_{\text{-Vmax}}$, $R_{\text{-CL}}$, $R_{\text{-Content}}$, referring to relative V_{max}, CL and Content, respectively, were computed to make CYP2A6 phenotypes at different levels comparable. Each level's relative V_{max}, CL and Content ($R_{\text{-Vmax}}$, $R_{\text{-CL}}$ and $R_{\text{-Content}}$) were calculated as the individual V_{max}, CL and Content divided by the median of corresponding parameter for that level.

Molecular level, or phenotype at the protein level, $V_{max\text{-}P}$ (pmol/min/pmol), $CL_{\text{-}P}$ (µl/min/pmol).

Sub-cellular level, or phenotype at microsomal level, $V_{max\text{-}M}$ (pmol/min/mg), $CL_{\text{-}M}$ (µl/min/mg), $Content_{\text{-}M}$ (pmol/mg).

Tissue level, or phenotype at liver tissue level, $V_{max\text{-}LT}$ (pmol/min/g), $CL_{\text{-}LT}$ (µl/min/g), $Content_{\text{-}LT}$ (pmol/g).

Organ level, or phenotype at liver level, $V_{max\text{-}L}$(nmol/min/kg), $CL_{\text{-}L}$ (µl/min/kg), $Content_{\text{-}L}$ (nmol/kg).

Organism level, or phenotype (clearance) at *in vivo* level, $CL_{\text{-}H}$ (ml/min).

[a]$P<0.05$ vs $V_{max\text{-}P}$ at Molecular level; [b]$P<0.05$ vs $V_{max\text{-}M}$ at Microsomal level; [b]$P<0.05$ vs $V_{max\text{-}LT}$ at Tissue level.

JPET Fast Forward. Published on December 27, 2019 as DOI: 10.1124/jpet.119.263152
This article has not been copyedited and formatted. The final version may differ from this version.

Figure 1

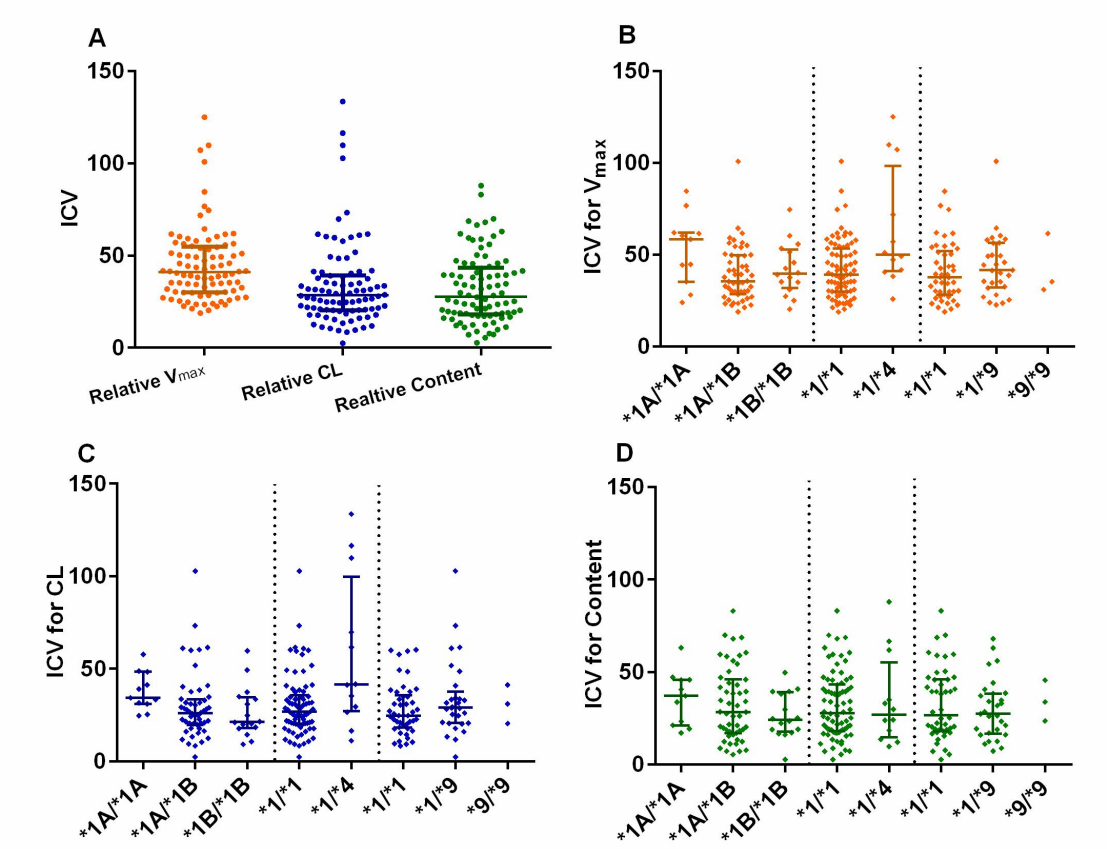

JPET Fast Forward. Published on December 27, 2019 as DOI: 10.1124/jpet.119.263152
This article has not been copyedited and formatted. The final version may differ from this version.

Figure 2

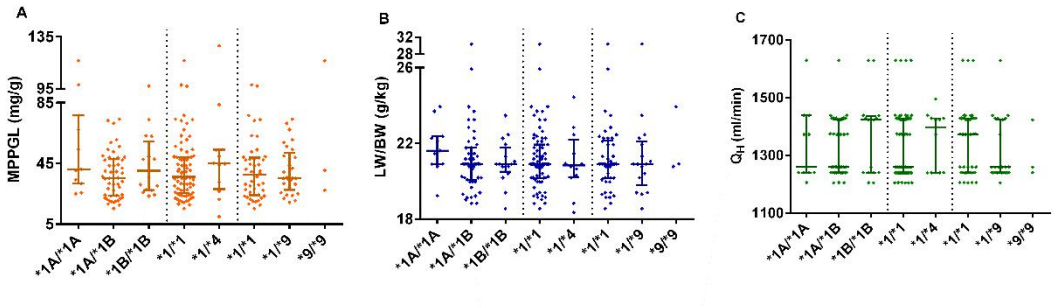

JPET Fast Forward. Published on December 27, 2019 as DOI: 10.1124/jpet.119.263152
This article has not been copyedited and formatted. The final version may differ from this version.

Figure 3

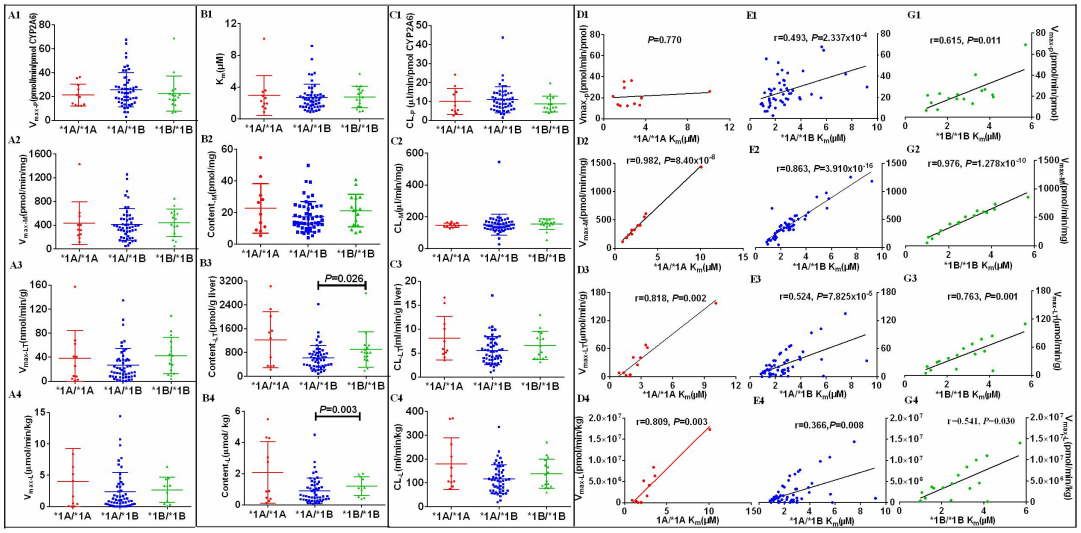

JPET Fast Forward. Published on December 27, 2019 as DOI: 10.1124/jpet.119.263152
This article has not been copyedited and formatted. The final version may differ from this version.

Figure 4

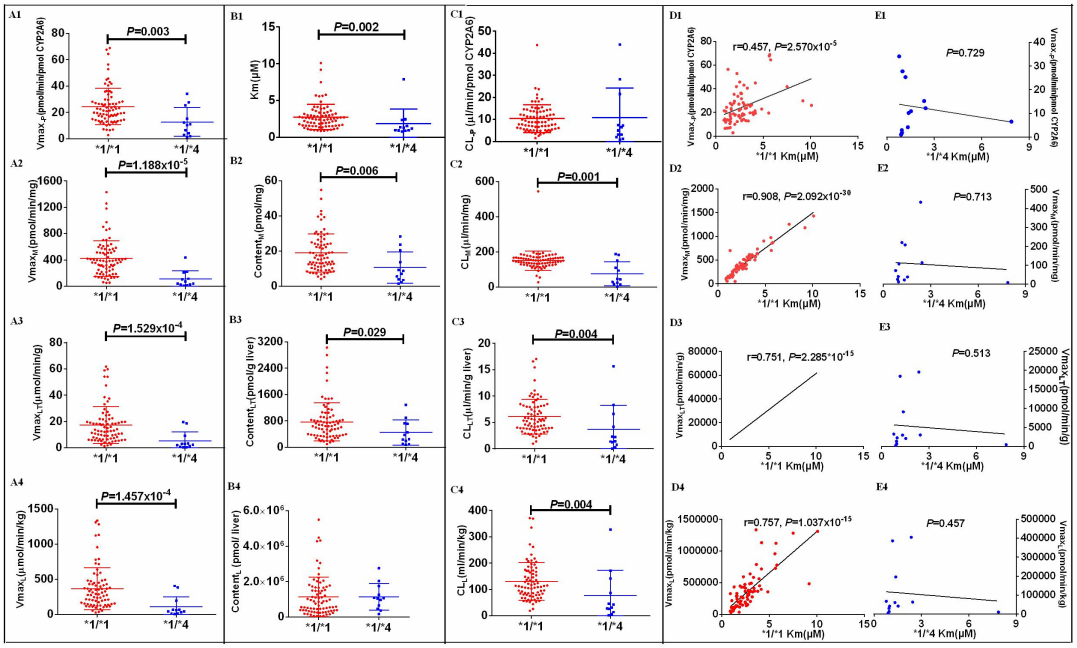

JPET Fast Forward. Published on December 27, 2019 as DOI: 10.1124/jpet.119.263152
This article has not been copyedited and formatted. The final version may differ from this version.

Figure 5

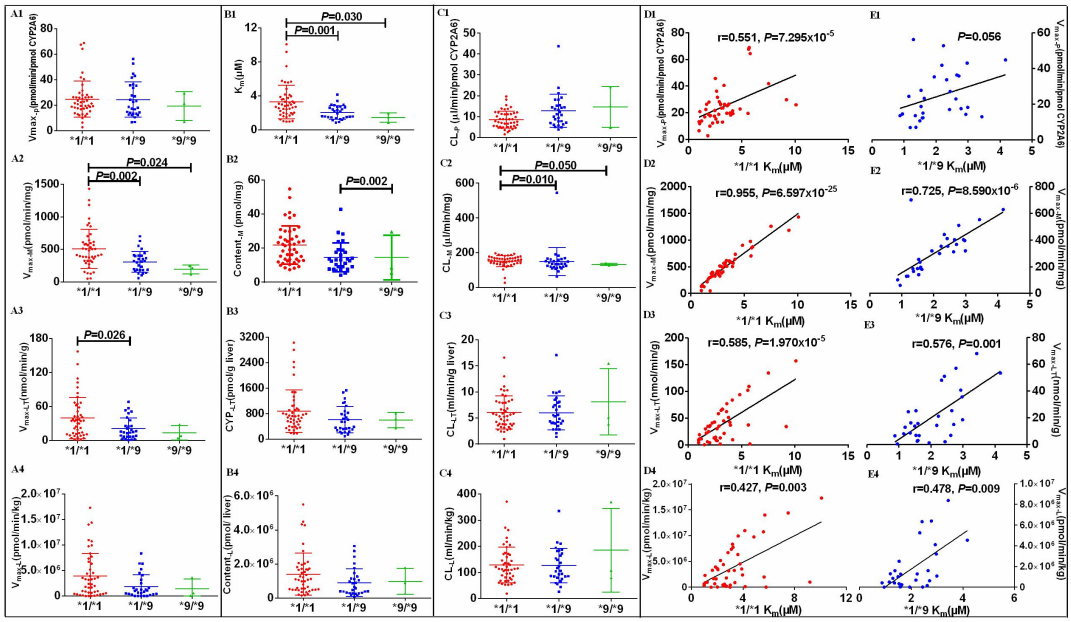

JPET Fast Forward. Published on December 27, 2019 as DOI: 10.1124/jpet.119.263152
This article has not been copyedited and formatted. The final version may differ from this version.

Figure 6